PCCP

Cite this: *Phys. Chem. Chem. Phys.*, 2017, **19**, 3845

The dynamic binding of cholesterol to the multiple sites of C99: as revealed by coarse-grained and all-atom simulations†

www.rsc.org/pccp

Introduction

The amyloid-β (Aβ) peptide is thought to play a key pathogenic role in Alzheimer's disease (AD), a disease showing progressive cognitive decline. The aggregation of amyloid-β (Aβ) peptides constitutes the main ingredients of neuritic plaques, which are pathologically characterized within the gray matter of the brain of AD patients.[1–4]

Aβ is cleaved by γ-secretase from C99, the 99 residues in the C-terminal domain of the amyloid precursor protein (APP), which is generated upon the cleavage of APP by β-secretase. A large body of evidence has shown that elevated levels of cholesterol (CHOL) promote the amyloidogenic pathway (the process of the formation of C99 from APP, mediated by β-secretase), resulting in increased levels of amyloid-β production and inhibition of the competing nonamyloidogenic cleavage pathway (in this route, APP is cleaved by α-secretase, then produces C83, which precludes the formation of C99 and Aβ) (Scheme 1).[5–14] Additionally, studies with purified γ-secretase have shown a 2- to 4-fold enhancement in the rates of production of both Aβ40 and Aβ42 in the presence of cholesterol with optimal levels of 5–20 mol%, depending on vesicle composition.[15]

With regard to the possible association between C99 and CHOL, this phenomenon can be explained by two hypotheses: (1) the specific interactions between C99 and cholesterol tend to allocate C99 and APP into cholesterol-rich membrane domains known as lipid rafts,[16,17] with which β-secretase and γ-secretase preferentially associate.[18–23] (2) The association between C99 and

[a] State Key Laboratory of Microbial Metabolism and College of Life Sciences and Biotechnology, Shanghai Jiao Tong University, Minhang District, Shanghai 200240, China. E-mail: xuqin523@sjtu.edu.cn, dqwei@sjtu.edu.cn
[b] Beijing Key Laboratory of Bioprocess, College of Life Science and Technology, Beijing University of Chemical Technology, Beijing, P. R. China
[c] Centre for Molecular Simulation and Department of Biological Sciences, University of Calgary, 2500 University Drive, N.W., Calgary, Alberta T2N 1N4, Canada

† Electronic supplementary information (ESI) available: The binding conformation, residue contribution and hydrogen bond of each binding site are depicted in the ESI. Figures and Tables are presented in the ESI. See DOI: 10.1039/c6cp07873g

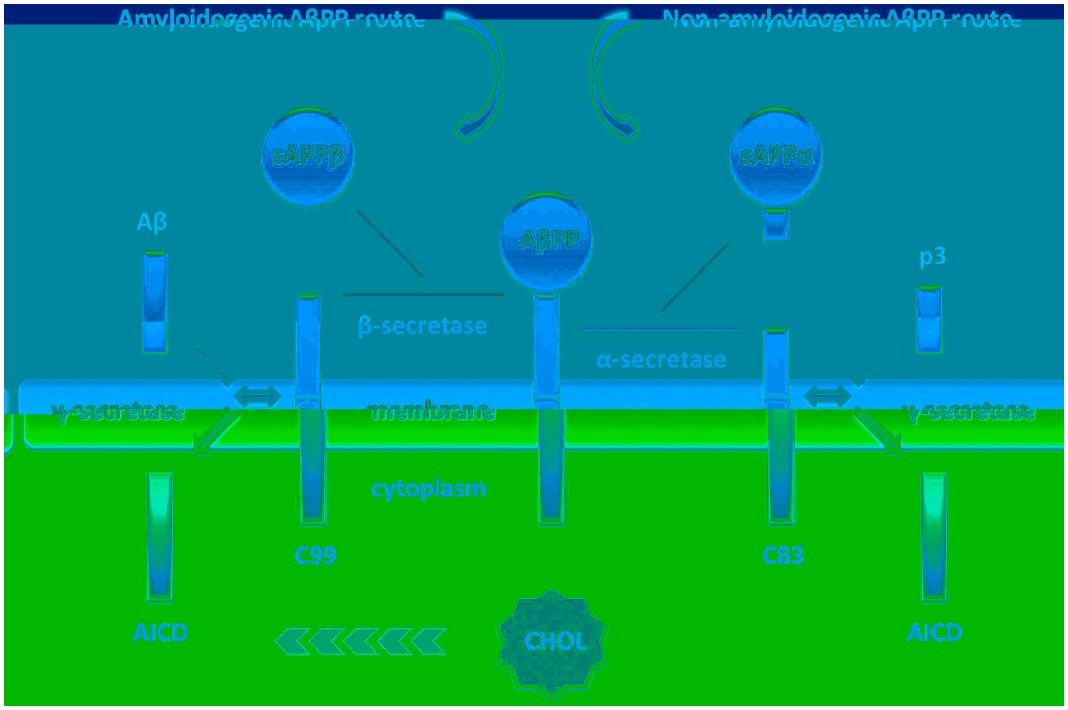

Scheme 1

cholesterol directly promotes the amyloidogenesis by helping C99 bind to γ-secretase.[24]

In the research by Barrett and his colleagues,[16,24] they put forward a cholesterol binding C99 model where cholesterol forms a 1 : 1 binary complex with monomeric C99 at the repeat GxxxG motif, and this complex competes with the C99 dimer. Mutation of any Gly residue or Phe_{691} or Glu_{693} to Ala substantially diminished cholesterol binding. This surprising observation strongly supports the above hypotheses, and hints at a significant functional effect of cholesterol on C99 dimerization and γ-cleavage. Subsequently, Lukasz Nierzwicki et al. accurately described the structure and energetics of the 1 : 1 complex identified by Barrett's NMR experiments, which suggests the existence of two different binding states at the GxxxG motif.[25] Recently, Straub et al. revealed that binding of cholesterol to the C99 GxxxG motif is a sensitive function of the pH, and is heavily dependent on the charge states of Glu_{693} and Asp_{694}.

Straub and Nierzwicki et al. have both simulated the 1 : 1 complex identified by Barrett's NMR experiments as the initial structure, since they were mainly aimed at the study of cholesterol binding at the GxxxG motif of C99. Nevertheless, the obtained results are significantly affected by the initial structure if the time scale of the simulation is limited. It raises the question of how the cholesterol binding occurs and if there are other binding sites that were neglected.

To observe the broader landscape of the association between C99 and cholesterol, in this study, a multi-scale computational approach was employed combining coarse-grained (CG) and all-atom (AT) simulations of the C99 monomer (based on the PDB structure 2LP1) in the DPPC : CHOL = 4 : 1 bilayer.

To assess the longtime dynamics and the role of fluctuations in the protein and lipid conformational ensemble,[26–28] CG simulations were performed for 10 × 3 μs using the MARTINI force field[29–31] to obtain more sampling, while AT simulation was performed for 1 μs using the CHARMM36 force field to obtain more accurate forecasts for the association between C99 and cholesterol.

Models and methodology

The experimentally derived NMR structure (PDB 2LP1[16]) was employed as the initial structure of the C99 monomer. Here, the protein sequence of $C99_{683–728}$ is VHHQKLVFFAEDVGSNK GAIIGLMVGGVVIATVIVITLVMLKKKQW, in which V_{683}HHQKL VFFAEDVGSNK$_{699}$ was defined as the juxtamembrane region, G_{700}AIIGLMVGGVV$_{711}$ was defined as the N terminus of C99 TMD, and I_{712}ATVIVITLVML$_{723}$ was defined as the C terminus of C99 TMD. The GxxxG motif here refers to the G_{696}xxxG_{700}xxxG_{704}xxxG_{708} zipper region.

CG

The Martinize.py script was used to create protein topology information, and the CG simulations were performed under the MARTINI 2.2 force field.[29] The insane.py script[32] was employed to build the DPPC : CHOL = 4 : 1 CG lipid systems (size = 8 × 8 nm^2), which contain 20% cholesterol levels (where mol% cholesterol = 100[moles cholesterol/(moles DPPC + moles cholesterol)]) to match the optimal concentration in Song' experiments.[24] The filling of cholesterol was consistent in the upper and lower layers. The monomer was then placed within the pre-equilibrated

lipid systems. The CG bilayer system consisted of C99 monomer, 120 DPPC lipids, 30 cholesterol molecules, 3863 water particles, and 3 Cl^- ions to neutralize the system.

All CG systems experienced the following three steps: energy minimization, NVT and NPT equilibration, and the molecular dynamics balance. The energy of each system was repeatedly minimized followed by 3 ns position-restrained simulation for better packing of the lipid molecules around the TM (transmembrane) helices. 10 replicas of 3 μs CG simulations were performed on each system in consideration of sample stability. Multiple independent dynamical trajectories were initiated from the experimentally determined 2LP1 PDB structure.

The temperature of the systems was set to 300 K using the Berendsen weak coupling method[33] with a relaxation time of 0.1 ps. The pressure was set to 1 bar using a semi-isotropic coupling for a bilayer using the Berendsen algorithm. An integration time step of 20 fs was used in all simulations. Nonbonded interactions were truncated using shift functions (between 0.9 and 1.2 nm for Lennard-Jones interactions and between 0 and 1.2 nm for electrostatics).[30]

R r CG

To explore a possible cholesterol binding model of C99, restrained simulations of an equilibrated C99 conformation, which was obtained from CG simulations and reached the platform period of RMSD (Fig. S2, ESI†), were performed in DPPC : CHOL = 4 : 1; where the position of protein atoms was limited by the harmonic potential with the force constant of 1000 kJ mol^{-1} nm^{-2} on each atom of the whole protein in the X, Y and Z directions. During the simulations, the protein is almost stationary with tiny harmonic vibration of the side chains. The other physiological conditions and simulation parameters of the protein restrained simulations are the same as the above CG model simulations.

AT

The AT model was constructed using the CHARMM-GUI Membrane Builder.[34] The final system is composed of a C99 fragment (Val683–Tyr728), 120 DPPC molecules, 30 cholesterol molecules, 5090 water molecules, 15 K^+ and 18 Cl^- ions (0.15 M). Proteins and lipids were presented using the CHARMM36 force field,[35] and a TIP3P model[36] was used for water. The NMR structure (PDB 2LP1[16]) was employed as the initial configuration of C99. The AT simulation system experienced the following three steps: energy minimization, NVT and NPT equilibration, and the molecular dynamics simulation. The temperature was set to 300 K by means of Langevin dynamics and the pressure was maintained at 1 bar using the Langevin piston method.[37] Periodic boundary conditions were employed, and the particle mesh Ewald algorithm was applied in full electrostatics with a real-space cut-off of 10 Å.[38] van der Waals interactions were truncated using shift functions between 10 Å and 12 Å. All covalent bonds including hydrogen were restrained by the LINCS method.[39] An integration time step of 2 fs was used in 1 μs AT simulation using the velocity Verlet algorithm.[40]

B r

g_mmpbsa[41,42] was used to evaluate binding energies as well as estimate the energy contribution of each residue to the binding energy. The binding energy is calculated based on the equation: $\Delta G_{bind} = \Delta E_{MM} + \Delta G_{psolv} + \Delta G_{npsolv} - T\Delta S$. ΔE_{MM} is the sum of van der Waals and electrostatic interactions. The entropy contribution ($T\Delta S$) is not calculated in g_mmpbsa, so this binding energy is the relative binding energy rather than the absolute binding energy.[43] All energy components of binding energies for the binding complex were calculated at every 500 ps interval from the 10 ns production trajectory (cut out from the 1 μs AT simulations) where the binding conformation is relatively stable. In this study, ΔE_{MM} contribution of each residue was employed to evaluate the residue contribution, as it is comparable to the binding energy.

All simulations were carried out using GROMACS (v4.6.1), and the analysis was performed using the GROMACS package, CG tailored scripts using python and CG analysis libraries.[44–48] Images were generated using VMD.[49] Detailed simulations are listed in Table S1 (ESI†).

Results and discussion

T C- r N- r C99 r r r

Tracking each cholesterol molecule near C99 monomer in all independent dynamical trajectories and analyzing the COM distance between the cholesterol and C99 monomer, no cholesterol molecule was found to keep a stable distance with the C99 monomer below 1 nm throughout the trajectory (Fig. 1A), which indicates that C99 cannot form 1 : 1 stable binding with cholesterol. But multiple COM distances within 1 nm in a short time about the 10–100 ns level were observed (Fig. 1A); this suggests that C99 might have short time interactions with cholesterol. In the CG trajectories, C99 is just like a flower with multiple bees of cholesterol molecules dynamically circling around, binding to and flying away from time to time. The flip-flop of cholesterol molecules over the upper and lower layers occurs infrequently during the simulations.

The cholesterol density distribution presents statistical aggregations of cholesterol molecules around the protein with a radial distance of about 0.5 nm in the upper and lower leaflets (Fig. 1B). This result clearly suggests that both the C-terminus and the N-terminus of C99 have interactions with cholesterol. And it is similar to Anupam Prakash's result about ebrB2,[50] which also presents a cholesterol surrounding model but with a more symmetrical distribution compared with C99 (Fig. S1, ESI†). The more pronounced aggregation of cholesterol in the C-terminus of C99 TMD reflects that the C-terminus might have more abundant interaction with cholesterol than the N-terminus, which can also be reflected in the cholesterol surrounding model (Fig. 2A).

However, we can hardly tell the cholesterol binding sites from this surrounding model due to the dynamics of the protein. In order to obtain the possible binding sites of C99, an equilibrated

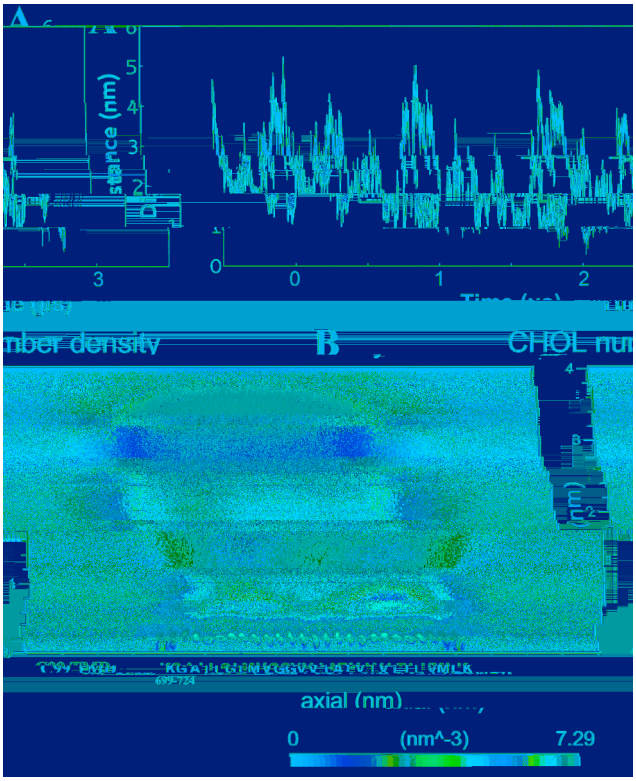

Fig. 1

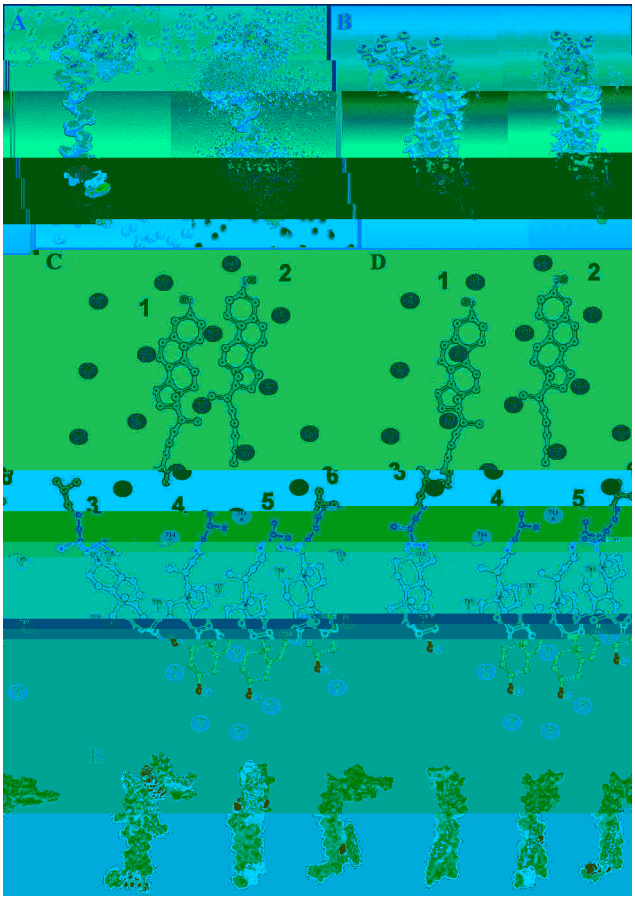

Fig. 2

2LP1 structure derived from the CG trajectory was employed in protein position-restrained CG simulation, and the results which were based upon the selected stable C99 structure were then further validated by the AT simulations where the flexibility of the protein and the C99-cholesterol interactions can be described more accurately.

A - r r

The isosurface of cholesterol in protein-restrained CG simulations (Fig. 2B) depicts 6 possible binding sites in the C99 TMD (transmembrane domain): two of which are in the N-terminus including the GxxxG motif, and the other four in the C-terminus (Fig. 2B and C). All binding sites located in the groove between two contact surfaces are concave for the anchorage of cholesterol (Fig. 2B and C). Cholesterol adjusts conformations to fit the different shapes of the binding sites. The cholesterol binding is constantly changing in forms of multiple binding, singular binding and no binding.

The results above are instructive, since all the binding sites found in restrained CG simulations have been screened out in the AT trajectories (Fig. 2E), according to the following standards: (1) cholesterol is closely attached to the protein surface; (2) cholesterol binds in the same area, which can be identified with residues as the scale; and (3) the combination time reaches the level of 10 ns. This suggests that those binding sites found in restrained CG simulations do exist. And it is feasible that protein restrained CG simulations can be performed as a preliminary search scheme of binding sites, complementary to detailed AT simulations.

Additionally, site 0 which is not fully reflected in the cholesterol isosurface (Fig. 2B) has been found, and it may be an intermediate state for cholesterol binding to site 1 (Fig. 3E). It is worth mentioning that the backbone conformation of the C99 TM in CG or AT simulation is consistent, which provides a theoretical basis for the similarities of the cholesterol binding sites in the two simulations. However, the binding positions of cholesterol at sites 1, 3 and 6 are slightly different from those in

the restrained CG model (Fig. 2C and D), as the protein structure in AT simulations is more dynamic and flexible compared to that in the semi-rigid protein restrained CG simulations, which result in shrinkage or deformation of the groove. Moreover, in CG simulations, the juxtamembrane region of C99 swings all the way, and the orientation of juxtamembrane along the membrane surface constantly changes. While, this orientation are relatively

two steps: firstly, juxtamembrane regions of C99 stretch and take the pistol-like Phe_{690} away from the GxxxG motif, leaving a pocket space for the cholesterol to anchor (Fig. 3A and B). In the meantime, the cholesterol cruises into the pocket, and the juxtamembrane region of C99 retracts with the side chain of Phe_{690} clamping the cholesterol tightly. Thus, cholesterol binding at the GxxxG motif occurs (Fig. 3C and D), where the head of cholesterol faces the Phe_{690}, forming a hydrogen bond throughout the binding (Fig. 3D and Table S2, ESI†), and the cholesterol methyl ring binds closely to the broad GxxxG motif (Fig. 3D and E). Phe_{690}, Gly_{704}, Ala_{701}, Leu_{705}, Gly_{708}, Val_{711}, Ile_{712} and Val_{715} contribute most to this loosely binding state with a binding energy of ~ -56.964 (Fig. S4, ESI†).

While Glu_{693} and Phe_{691}, the key residues in the 1 : 1 binary complex proposed by Barrett,[51] have little contact with cholesterol in our results where Phe_{690} is prominent instead (Fig. S4, ESI†). In fact, Straub et al. have explained that Barrett's NMR experimental data were collected at pH 4.5, which results in the protonation of Glu_{693} and Asp_{694} (natural pK_a values of Glu and Asp side chains are 4.4 and 4.0 respectively), and leads to the insertion of Glu_{693} and Asp_{694} in the membrane interior together with Phe_{691}. Under a neutral pH, Glu_{693}, Asp_{694} and Phe_{691} shift toward the membrane exterior; thus, no significant contacts were observed between cholesterol and these three residues.[52] This description by Straub is in agreement with our observation.

It is interesting to point out that the escape of the cholesterol from the GxxxG binding site is also very difficult. When the cholesterol fights to escape from the pocket of site 1, it has to trek through the bulge of Phe_{690}. Even if it succeeds, cholesterol will quickly encounter the second barrier Lys_{687} which will strongly attract it via the hydrogen bond (Fig. 3E and F and Table S2, ESI†), and the flexible tail of cholesterol can hardly resist the temptation of the hydrophobic residues Ile_{712} and Val_{711}. The binding state at site 0 with binding energy ~ -15.999 kJ mol^{-1} (Fig. 3F and Table 1), which the residues Lys_{687}–Phe_{690} contribute most to (Fig. S3, ESI†), is the most appropriate for the escape of the cholesterol. Otherwise, the Phe_{690} turns sideways and the juxtamembrane region of C99 retracts close to the GxxxG motif in the meantime. In this way, cholesterol will be sent back to the GxxxG motif and experiences the loosely binding state again (Fig. 3F and G). Therefore, there are two pathways by which cholesterol binds to the GxxxG motif: from Fig. 3B to C, or Fig. 3F to G. The difficult process of cholesterol binding to or disassociation from the GxxxG motif may suggest site 1 to be a kinetically unfavorable site for cholesterol binding, while the relatively strong binding energy may suggest it to be a thermodynamically favorable site. In a general reaction process, the molecule needs to overcome an energy barrier to reach the favorable energy binding sites; while a greater energy barrier should be overcome in the reverse dissociation reaction.

It is surprising that the structure of C99 could be further optimized in the loosely binding state: the N-loop expands, allowing cholesterol to access the bottom of the pocket, where Ser_{697} forms a strong hydrogen bond with the cholesterol head (Fig. 3G and H and Table S2, ESI†). The residues Ser_{697}, Ala_{701}, Val_{711}, and Ile_{712} and all the four Gly residues of $G_{696}xxxG_{700}xxxG_{704}xxxG_{708}$ zipper motifs contribute most to this tightly binding state (Fig. S4, ESI†). It is more dynamically stable than the loosely binding state: ~ -58.857 binding for the tightly binding state and ~ -56.964 for the loosely binding state.

The above observation is in agreement with the description by Łukasz Nierzwicki et al. that there exist two binding states at the GxxxG motif, whose free energies are almost equal. The interactions between the GxxxG motif and the cholesterol rings are not sufficient for binding.[25] In the tightly binding state, the cholesterol methyl ring associates intimately with the GxxxG motifs of C99. The loosely binding state is stabilized primarily by the interactions between the 3′-hydroxyl group and the A ring of cholesterol with the juxtamembrane of C99.[25] Additionally, more details were revealed in our simulations. In the tightly binding state, the cholesterol is largely stabilized by Ser_{697} in the juxtamembrane of C99; while in the loosely binding state, Phe_{690} plays a key role in the stabilization of cholesterol binding (Fig. S4, ESI†).

T r r r

As regards site 5, whose binding energy is nearly -54.725 kJ mol^{-1} (Table 1 and Fig. S8, ESI†), the dynamic process is relatively simple. The groove between two contact surfaces has been an empty seat for cholesterol before its arrival. Cholesterols adhere to the protein surface like flies with the protein dynamics, as if protein shivers with itching but cannot shake off the cholesterol. The long side chain of $Lys_{725-727}$ residues is cross-arranged like the lotus base holding the head of cholesterol (Fig. S8 and Table S2, ESI†), which has a similar role to that in the complex: cholesterol-binding Aβ.[53] The residues Val_{710}, Ile_{712}, Ala_{713}, Ile_{716}, Val_{717}, Leu_{720} and Lys_{726} contribute most to the binding (Fig. S8, ESI†).

The processes of cholesterol binding to other sites are roughly similar to that at site 5 but with different binding strengths (Table 1 and Fig. S3–S9, ESI†). In fact, there are also more superficial and shorter time contacts of cholesterol with protein. Even when cholesterol binds to these relatively stable sites above, it is not completely fixed; it adopts a corresponding fine-tuning in the binding area together with the dynamic movement of the protein. The types of cholesterol binding can be divided into two categories: the β surface binding (the apposed α face is smooth, while the β surface is relatively rough) and side surface binding. "The β surface of cholesterol has two methyl groups (C18 and C19) protruding out of the plane of the sterol ring. These methyls can serve as knobs to fit in grooves or holes in the protein surface".[54] On the other hand, the binding sites can also be divided into two kinds according to the binding position: the groove binding and the ridge binding. The groove binding was observed at sites 1, 2, 4 and 5; (Fig. 4 and Fig. S3–S9, ESI†), where cholesterol tends to bind in the groove space with the β surface and switch to side surface binding when the groove space shrinks (Fig. 4). In contrast, cholesterol often binds the ridge with the side surface at site 3 and site 6 (Fig. S6 and S9, ESI†). In particular, in our 1 μs AT simulations, no matter in a loosely binding state or tightly binding state at the GxxxG motif,

cholesterol mostly interacts with the GXXXG motif in side surface binding. This is different with Straub's observation that cholesterol prefers α surface binding with the GxxxG motif,[52] which may be related to the initial location of the cholesterol in the 1 : 1 binary complex. The binding conformations, hydrogen bonds and r[illegible]e contribution at each site are also provided in the ESI† (Fig[illegible]S9 and Table S2).

T[illegible]KF, IKF r

The summar[illegible]f residue contributions to the ΔMM energy (Fig. 5) shows[illegible]t the high contribution residues are, respectively, Phe_{690}, Lys_{69}[illegible]le_{702}–Met_{706}, Gly_{708}, Val_{710}–Ile_{718} and Lys_{725}; in which Phe[illegible] Lys_{699}, Ile_{712}, Val_{717} and Lys_{725} are particularly outstanding. [illegible]hile Leu, Gly and Ala are essential to some binding sites. [illegible]detailed description of residue contribution to each binding [illegible]s is provided in the ESI.† Given the cholesterol's hydrophobici[illegible]the result is of no surprise as e resid354.3(6)21tion(r)19.20.6(-250.7(in)]TJ0-1.35(e.4(u)hole5.4on(r)(e.4(u)0(r)pJT[h(r)a8.9(5(,)-2

In our results, six binding sites were presented, where the residue IVLGAMTKF plays a key role. The sequences of these binding sites bear great similarity to the consensus above, especially for the binding sites containing the Lys residue. Differently, these binding sites do not involve the aromatic residue. In fact, in the study regarding the CRAC of the TM5 domain of human type 3 somatostatin receptor, Jacques Fantin et al. explained that the central Y-226 residue is not involved in the interaction.[73] Additionally, fusogenic tilted peptides can interact with cholesterol, although they do not contain the central residues.[68] On the other hand, Fantin et al. have illustrated that the TM domain, which contains both a CRAC and a CARC sequence, can allow the simultaneous binding of two cholesterol molecules.[73] Moreover, the energetic pattern of the cholesterol binding site, 221-_ICL**C**YL**L**IVVK**K**-232 (note: residues involved in cholesterol binding are underlined and in bold), do not overlap with any of the two CRAC motifs (**L**C_LLIVV**K** or ICLC LLIVV**K**).[73] These results support the establishment of multiple binding in the same sequence.

The C99 model appears to suggest a new interpretation for cholesterol binding. It is believed that cholesterol binding is not only dependent upon simple residue effects but also greatly upon the appropriate structural domains with which cholesterol chooses a flexible conformation to fit. Another reason for cholesterol binding, to a larger extent is due to hydrogen bonding between specific amino acids and cholesterol's hydroxyl head groups. For integral membrane proteins, the hydrogen bonding has, so far, always been located near the water–membrane interface.[54] It is plausible that the essence of cholesterol binding is to bind the head of cholesterol by the hydrogen bond with residues Lys or Phe and bind the methyl ring and isooctyl tail of cholesterol by van der Waals interactions with an appropriate structural domain consisting of aliphatic amino acids (Gly, Ala, Val, Ile, Leu, Met and Thr). For the monomer–cholesterol interfaces, entropy should be considered. The association between the cholesterol and the protein is favored in terms of entropy, since the formation of the rigid and flat surfaces by cholesterol binding somehow dampened the protein dynamic motions, their surfaces would be less solvated in a fluid phase membrane.[69,70]

Overall, cholesterol has a wide association with a variety of proteins, and that there is a consensus of sequences in association with cholesterol. The specific model depending on protein structures might be significant for the execution of physiological functions.[71,72]

In summary, the association between cholesterol and C99 is a dynamic and multi-site interaction characterized by molecular simulation, and it plays a special role in the amyloidogenic pathway. There are still many issues, which need to be studied in further detail.

Conclusions

Both the N-terminus and the C-terminus of C99 show interactions with cholesterol, which leads to multiple binding modes rather than the one stable binding mode. The multi-site dynamic cholesterol binding model was captured based on an equilibrated C99 conformation and has been further validated by AT simulation. In this model, there are six regions of cholesterol binding in the C99 TMD (transmembrane domain): two of which are in the N-terminus including the repeat GxxxG motif, and the other four in the C-terminus. The analysis of binding energy shows that cholesterol prefers the sites: no. 1, 2, 4 and 5 over others. The most favorable binding energy of nearly -58.857 kJ mol^{-1} is from site 1, the repeat GxxxG motif, and there are two pathways and two states of cholesterol binding to this site. Ser_{697} and the Phe_{690} contribute the most in the stabilization of a tightly binding state and a loosely binding state, respectively. The type of cholesterol binding can be divided into two categories: the β surface binding and side surface binding. On the other hand, the binding sites can also be divided into two kinds according to the binding position: the groove and convex binding sites. The association of cholesterol is commonly found within a variety of proteins, and the residue GAVILMTKF, particularly VIKF, plays a key role in this association. The C99 model appears to suggest a new mechanism for cholesterol binding. It is plausible that the essence of cholesterol binding is to bind the head of cholesterol by hydrogen bond with the residue Phe or Lys and bind the isooctyl chain and the methyl ring of cholesterol by van der Waals interactions with an appropriate structural domain consisting of aliphatic amino acids (GAVILMT). Compared with a single cholesterol stable binding model, the multi-site dynamic cholesterol binding model of C99 better explains the hypotheses that cholesterol promotes the amyloidogenic AβPP route. The backbones of the $G_{709}xxxA_{713}$ motif are completely exposed without a cholesterol shelter, which might help γ-secretase identify the cleavage sites and then promote γ-cleavage.

Competing financial interest

The authors declare no competing financial interest.

Funding sources

Dong-Qing Wei was supported by grants from the National High-Tech R&D Program (863 Program Contract No. 2012AA020307), the National Basic Research Program of China (973 Program) (Contract No. 2012CB721000), and PhD Programs Foundation of Ministry of Education of China (Contract No. 20120073110057). Qin Xu was supported by grants from the National Natural Science Foundation of China for Young Scholars (Grant No. 31400704). Dong-Qing Wei and Qin Xu were supported by the Key Research Area Grant 2016YFA0501703 from the Ministry of Science and Technology of China.

Acknowledgements

We are most grateful to Professor Shi-Zhong Luo for helpful discussions and valuable references he gave in the early stages of the work. We thank Hai-Yang Zhang for technical assistance and Yan-Yu Li for proofreading. The simulations in this work were supported by Center for High Performance Computing, Shanghai Jiao Tong University.

References

1 T. Iwatsubo, A. Odaka, N. Suzuki, H. Mizusawa, N. Nukina and Y. Ihara, Visualization of Aβ42(43) and Aβ40 in senile plaques with end-specific Aβ monoclonals: Evidence that an initially deposited species is Aβ42(43), Neuron, 1994, **13**, 45–53.

2 M. D. Kirkitadze, G. Bitan and D. B. Teplow, Paradigm shifts in Alzheimer's disease and other neurodegenerative disorders: The emerging role of oligomeric assemblies, J. Neurosci. Res., 2002, **69**, 567–577.

3 D. M. Walsh, I. Klyubin, J. V. Fadeeva, W. K. Cullen, R. Anwyl, M. S. Wolfe, M. J. Rowan and D. J. Selkoe, Naturally secreted oligomers of amyloid β protein potently inhibit hippocampal long-term potentiation in vivo, Nature, 2002, **416**, 535.

4 P. Seubert, C. Vigo-Pelfrey, F. Esch, M. Lee, H. Dovey, D. Davis, S. Sinha, M. Schiossmacher, J. Whaley, C. Swindlehurst, R. McCormack, R. Wolfert, D. Selkoe, I. Lieberburg and D. Schenk, Isolation and quantification of soluble Alzheimer's beta-peptide from biological fluids, Nature, 1992, **359**, 325–327.

5 S. Bodovitz and W. L. Klein, Cholesterol modulates α-secretase cleavage of amyloid precursor protein, J. Biol. Chem., 1996, **271**, 4436–4440.

6 K. Fassbender, M. Simons, C. Bergmann, M. Stroick, D. Lutjohann, P. Keller, H. Runz, S. Kuhl, T. Bertsch, K. Von Bergmann, M. Hennerici, K. Beyreuther and T. Hartmann, Simvastatin strongly reduces levels of Alzheimer's disease β-amyloid peptides Aβ42 and Aβ40 in vitro and in vivo, Proc. Natl. Acad. Sci. U. S. A., 2001, **98**, 5856–5861.

7 A. C. R. G. Fonseca, R. Resende, C. R. Oliveira and C. M. F. Pereira, Cholesterol and statins in Alzheimer's disease: Current controversies, Exp. Neurol., 2010, **223**, 282–293.

8 M. O. W. Grimm, H. S. Grimm, I. Tomic, K. Beyreuther, T. Hartmann and C. Bergmann, Independent inhibition of Alzheimer disease β- and γ-secretase cleavage by lowered cholesterol levels, J. Biol. Chem., 2008, **283**, 11302–11311.

9 C. Guardia-Laguarta, M. Coma, M. Pera, J. Clarimón, L. Sereno, J. M. Agulló, L. Molina-Porcel, E. Gallardo,

A. Deng, O. Berezovska, B. T. Hyman, R. Blesa, T. Gómez-Isla and A. Lleó, Mild cholesterol depletion reduces amyloid-β production by impairing APP trafficking to the cell surface, J. Neurochem., 2009, **110**, 220–230.

10 E. Kojro, G. Gimpl, S. Lammich, W. Marz and F. Fahrenholz, Low cholesterol stimulates the nonamyloidogenic pathway by its effect on the α-secretase ADAM 10, Proc. Natl. Acad. Sci. U. S. A., 2001, **98**, 5815–5820.

11 L. M. Refolo, M. A. Pappolla, J. LaFrancois, B. Malester, S. D. Schmidt, T. Thomas-Bryant, G. S. Tint, R. Wang, M. Mercken, S. S. Petanceska and K. E. Duff, A Cholesterol-Lowering Drug Reduces β-Amyloid Pathology in a Transgenic Mouse Model of Alzheimer's Disease, Neurobiol. Dis., 2001, **8**, 890–899.

12 H. Runz, J. Rietdorf, I. Tomic, M. de Bernard, K. Beyreuther, R. Pepperkok and T. Hartmann, Inhibition of intracellular cholesterol transport alters presenilin localization and amyloid precursor protein processing in neuronal cells, J. Neurosci., 2002, **22**, 1679–1689.

13 M. Simons, P. Keller, B. De Strooper, K. Beyreuther, C. G. Dotti and K. Simons, Cholesterol depletion inhibits the generation of β-amyloid in hippocampal neurons, Proc. Natl. Acad. Sci. U. S. A., 1998, **95**, 6460–6464.

14 S. Wahrle, P. Das, A. C. Nyborg, C. McLendon, M. Shoji, T. Kawarabayashi, L. H. Younkin, S. G. Younkin and T. E. Golde, Cholesterol-Dependent γ-Secretase Activity in Buoyant Cholesterol-Rich Membrane Microdomains, Neurobiol. Dis., 2002, **9**, 11–23.

15 P. Osenkowski, W. Ye, R. Wang, M. S. Wolfe and D. J. Selkoe, Direct and Potent Regulation of γ-Secretase by Its Lipid Microenvironment, J. Biol. Chem., 2008, **283**, 22529–22540.

16 P. J. Barrett, Y. Song, W. D. Van Horn, E. J. Hustedt, J. M. Schafer, A. Hadziselimovic, A. J. Beel and C. R. Sanders, The Amyloid Precursor Protein Has a Flexible Transmembrane Domain and Binds Cholesterol, Science, 2012, **336**, 1168–1171.

17 A. J. Beel, C. K. Mobley, H. J. Kim, F. Tian, A. Hadziselimovic, B. Jap, J. H. Prestegard and C. R. Sanders, Structural studies of the transmembrane C-terminal domain of the amyloid precursor protein (APP): does APP function as a cholesterol sensor?, Biochemistry, 2008, **47**, 9428–9446.

18 A. J. Beel, M. Sakakura, P. J. Barrett and C. R. Sanders, Direct binding of cholesterol to the amyloid precursor protein: An important interaction in lipid-Alzheimer's disease relationships?, Biochim. Biophys. Acta, Mol. Cell Biol. Lipids, 2010, **1801**, 975–982.

19 H. Cheng, K. S. Vetrivel, P. Gong, X. Meckler, A. Parent and G. Thinakaran, Mechanisms of disease: new therapeutic strategies for Alzheimer's disease-targeting APP processing in lipid rafts, Nat. Clin. Pract. Neurol., 2007, **3**, 374–382.

20 G. Di Paolo and T.-W. Kim, Linking lipids to Alzheimer's disease: cholesterol and beyond, Nat. Rev. Neurosci., 2011, **12**, 284–296.

21 D. A. Hicks, N. N. Nalivaeva and A. J. Turner, Lipid rafts and Alzheimer's disease: protein-lipid interactions and perturbation of signaling, Front. Membr. Physiol. Biophys., 2012, **3**, 189.

22 I. J. Martins, T. Berger, M. J. Sharman, G. Verdile, S. J. Fuller and R. N. Martins, Cholesterol metabolism and transport in the pathogenesis of Alzheimer's disease, J. Neurochem., 2009, **111**, 1275–1308.

23 J. V. Rushworth and N. M. Hooper, Lipid rafts: linking Alzheimer's amyloid-β production, aggregation and toxicity at neuronal membranes, Int. J. Alzheimer's Dis., 2011, 603014.

24 Y. Song, E. J. Hustedt, S. Brandon and C. R. Sanders, Competition Between Homodimerization and Cholesterol Binding to the C99 Domain of the Amyloid Precursor Protein, Biochemistry, 2013, **52**, 5051–5064.

25 L. Nierzwicki and J. Czub, Specific Binding of Cholesterol to the Amyloid Precursor Protein: Structure of the Complex and Driving Forces Characterized in Molecular Detail, J. Phys. Chem. Lett., 2015, **6**, 784–790.

26 G. S. Ayton and G. A. Voth, Systematic multiscale simulation of membrane protein systems, Curr. Opin. Struct. Biol., 2009, **19**, 138–144.

27 A. P. Lyubartsev and A. L. Rabinovich, Recent development in computer simulations of lipid bilayers, Soft Matter, 2011, **7**, 25–39.

28 H. L. Scott, Modeling the lipid component of membranes, Curr. Opin. Struct. Biol., 2002, **12**, 495–502.

29 L. Monticelli, S. K. Kandasamy, X. Periole, R. G. Larson, D. P. Tieleman and S.-J. Marrink, The MARTINI Coarse-Grained Force Field: Extension to Proteins, J. Chem. Theory Comput., 2008, **4**, 819–834.

30 S. J. Marrink, H. J. Risselada, S. Yefimov, D. P. Tieleman and A. H. De Vries, The MARTINI Force Field: Coarse Grained Model for Biomolecular Simulations, J. Phys. Chem. B, 2007, **111**, 7812–7824.

31 S. J. Marrink, A. H. de Vries and D. P. Tieleman, Lipids on the move: Simulations of membrane pores, domains, stalks and curves, Biochim. Biophys. Acta, Biomembr., 2009, **1788**, 149–168.

32 T. A. Wassenaar, H. I. Ingolfsson, R. A. Bockmann, D. P. Tieleman and S. J. Marrink, Computational Lipidomics with insane: A Versatile Tool for Generating Custom Membranes for Molecular Simulations, J. Chem. Theory Comput., 2015, **11**, 2144–2155.

33 H. J. C. Berendsen, J. P. M. Postma, W. F. Van Gunsteren, A. DiNola and J. R. Haak, Molecular dynamics with coupling to an external bath, J. Chem. Phys., 1984, **81**, 3684–3690.

34 S. Jo, J. B. Klauda and W. Im, CHARMM-GUI Membrane Builder for Mixed Bilayers and Its Application to Yeast Membranes, Biophys. J., 2009, **97**, 50–58.

35 J. Huang and A. D. MacKerell, Jr, CHARMM36 all-atom additive protein force field: Validation based on comparison to NMR data, J. Comput. Chem., 2013, **34**, 2135–2145.

36 W. L. Jorgensen, J. Chandrasekhar, J. D. Madura, R. W. Impey and M. L. Klein, Comparison of Simple Potential Functions for Simulating Liquid Water, J. Chem. Phys., 1983, **79**, 926–935.

37 S. E. Feller, Y. Zhang, R. W. Pastor and B. R. Brooks, Constant pressure molecular dynamics simulation: The Langevin piston method, J. Chem. Phys., 1995, **103**, 4613–4621.

38 T. Darden, Particle mesh Ewald: An N-log(N) method for Ewald sums in large systems, J. Chem. Phys., 1993, **98**, 10089–10092.
39 B. Hess, H. Bekker, H. J. C. Berendsen and J. G. E. M. Fraaije, LINCS: A linear constraint solver for molecular simulations, J. Comput. Chem., 2008, **4**

68 J. Fantini, D. Carlus and N. Yahi, The fusogenic tilted peptide (67–68) of α-synuclein is a cholesterol binding domain, Biochim. Biophys. Acta, 2011, **1808**, 2343–2351.
69 V. Helms, Attraction within the membrane. Forces behind transmembrane protein folding and supramolecular complex assembly, EMBO Rep., 2002, **3**, 1133–1138.
70 J.-L. Popot and D. M. Engelman, Helical membrane protein folding, stability, and evolution, Annu. Rev. Biochem., 2000, **69**, 881–922.
71 G. Gimpl, J. Reitz, S. Brauer and C. Trossen, Oxytocin receptors: ligand binding, signalling and cholesterol dependence, Prog. Brain Res., 2008, **170**, 193–204.
72 T. L. Steck and Y. Lange, Cell cholesterol homeostasis: mediation by active cholesterol, Trends Cell Biol., 2010, **20**, 680–687.
73 A. Fukumori, R. Fluhrer, H. Steiner and C. Haass, Three-amino acid spacing of presenilin endoproteolysis suggests a general stepwise cleavage of γ-secretase-mediated intramembrane proteolysis, J. Neurosci., 2010, **30**, 7853–7862.
74 S. Funamoto, M. Morishimakawashima, Y. Tanimura, N. Hirotani, T. C. Saido and Y. Ihara, Truncated Carboxyl-Terminal Fragments of β-Amyloid Precursor Protein Are Processed to Amyloid β-Proteins 40 and 42?, Biochemistry, 2004, **43**, 13532–13540.
75 M. Takami, Y. Nagashima, Y. Sano, S. Ishihara, M. Morishimakawashima, S. Funamoto and Y. Ihara, gamma-Secretase: successive tripeptide and tetrapeptide release from the transmembrane domain of beta-carboxyl terminal fragment, J. Neurosci., 2009, **29**, 13042–13052.

